Cell Reports, Volume *42*

Supplemental information

IGFBPL1 is a master driver of microglia homeostasis and resolution of neuroinflammation in glaucoma and brain tauopathy

Li Pan, Kin-Sang Cho, Xin Wei, Fuyi Xu, Anton Lennikov, Guangan Hu, Jing Tang, Shuai Guo, Julie Chen, Emil Kriukov, Robert Kyle, Farris Elzaridi, Shuhong Jiang, Pierre A. Dromel, Michael Young, Petr Baranov, Chi-Wai Do, Robert W. Williams, Jianzhu Chen, Lu Lu, and Dong Feng Chen

Supplementary Figures

Fig. S1

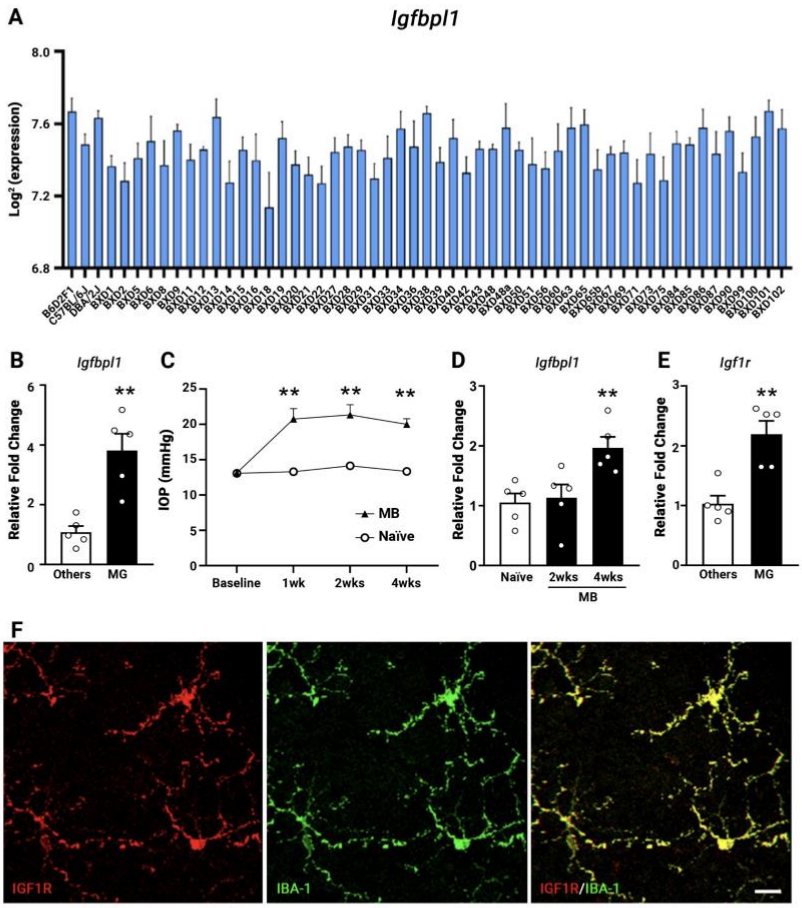

Figure S1. Genome-wide integrative analysis of IGFBPL1 in BXD and *Igfbpl1*$^{-/-}$ mice.

(A) Variation of mRNA levels of *Igfbpl1* across the BXD strains.

(B) qPCR quantification of *Igfbpl1* mRNA levels in retinal microglia (MG) *vs* all other retinal cells (Others). **p<0.01, Student's t test.

(C) IOP levels in naïve and microbead (MB)-injected mice. **p<0.01, Two-way ANOVA with Šídák multiple comparisons test.

(D) qPCR quantification of *Igfbpl1* mRNA levels in isolated microglia taken from naive mice and MB-injected mice at 2- and 4-weeks post IOP elevation. **p<0.01, One-way ANOVA with Dunnett's multiple comparisons test.

(E) qPCR result of *Igf1r* mRNA levels in retinal microglia (MG) *vs* all other retinal cells (Others). **p<0.01, Student's t test.

(F) Representative images of retinal flat-mount that were double-immunolabeled for IGF1R (red) and IBA-1 (green). Scale bar, 10 μm.

Data are from n= 5 mice per group. Dots represent individual mice. Data are mean ± SEM.

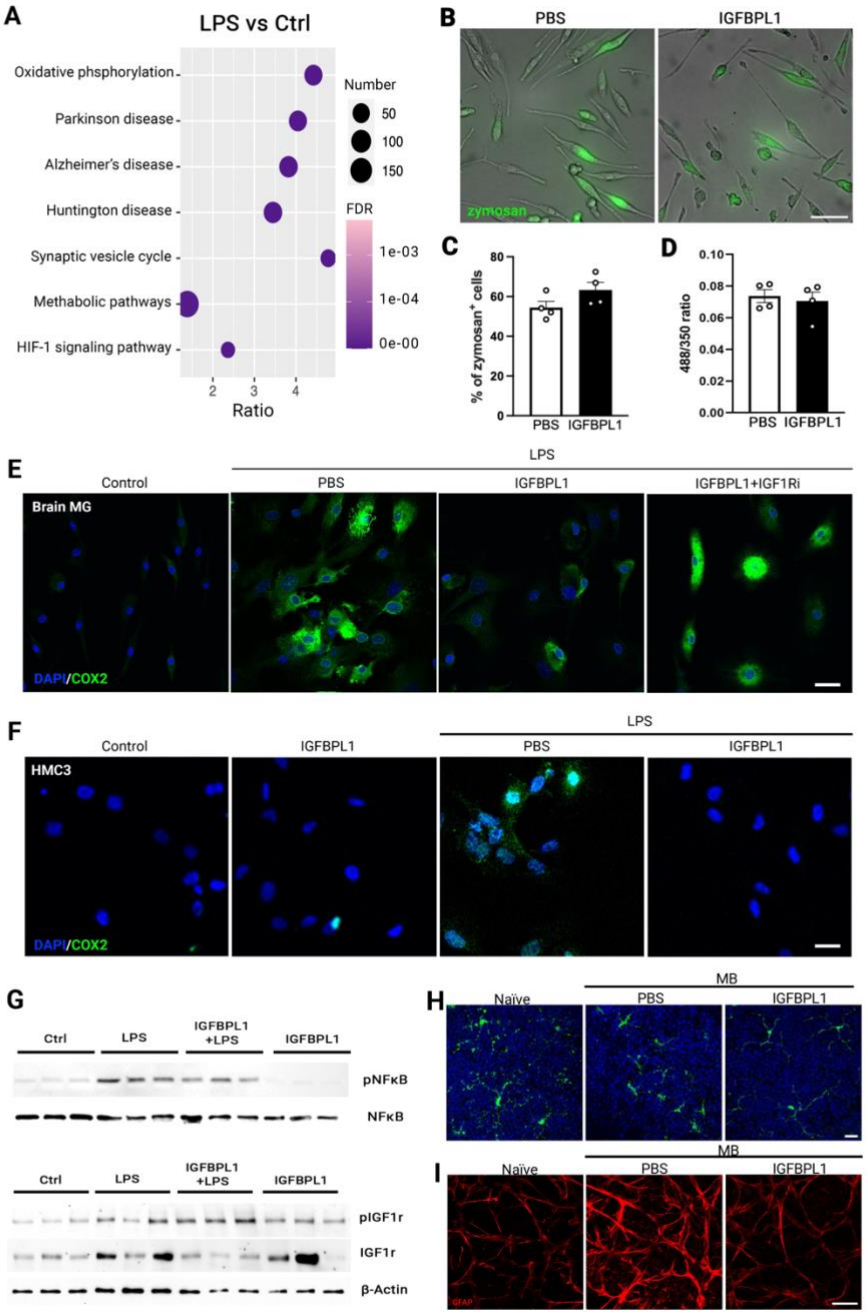

Figure S2. IGFBPL1 suppresses the activation of LPS-primed mouse brain microglia or human microglial cell line HMC3

(A) Dotplots of top 7 enriched KEGG pathway terms analyzed based on 2,163 DEGs between LPS-treated and control microglia (A). The x-axis represents the enrich ratio.

(B-D) Representative zymosan fluorescence images superimposed onto phase contrast (PC; B) and quantification of zymosan uptake (C) in PBS- and IGFBPL1-treated

microglial cultures. Percentage of cells with zymosan particles were determined using the 350/420 nm excitation/emission of hoechst nuclear staining (total cell number). and 485/520 nm excitation/emission of zymosan particles (D). *$p<0.05$, Student's t test. n=4. Scale bar, 50 μm.

(E and F) Representative images of primary brain microglia (E) and human HMC3 cells (F) immunolabeled for COX2 (green) and countered stained with DAPI (blue) in control, LPS, LPS+PBS, LPS+IGFBPL1, and LPS+IGFBPL1+IGF-1Ri treated cultures. Scale bar, 20 μm.

(G) Representative Western blots of pNFκB and pIGF1R in primary mouse microglial cultures treated with PBS control, LPS, IGFBPL1 or LPS with IGFBPL1 for 2 hr. n=3/group.

(H) Images of IBA-1^+ (green) cells with countered stained DAPI (blue) in retinal flat-mounts of naïve or MB-injected mice received PBS or IGFBPL1 treatment. Scale bar, 20μm

(I) Images of GFAP-immunolabeled retinal flat-mounts of naïve or MB-injected mice treated with PBS or IGFBPL1. Scale bar, 50μm.

Dots represent individual data. Data are mean±SEM.

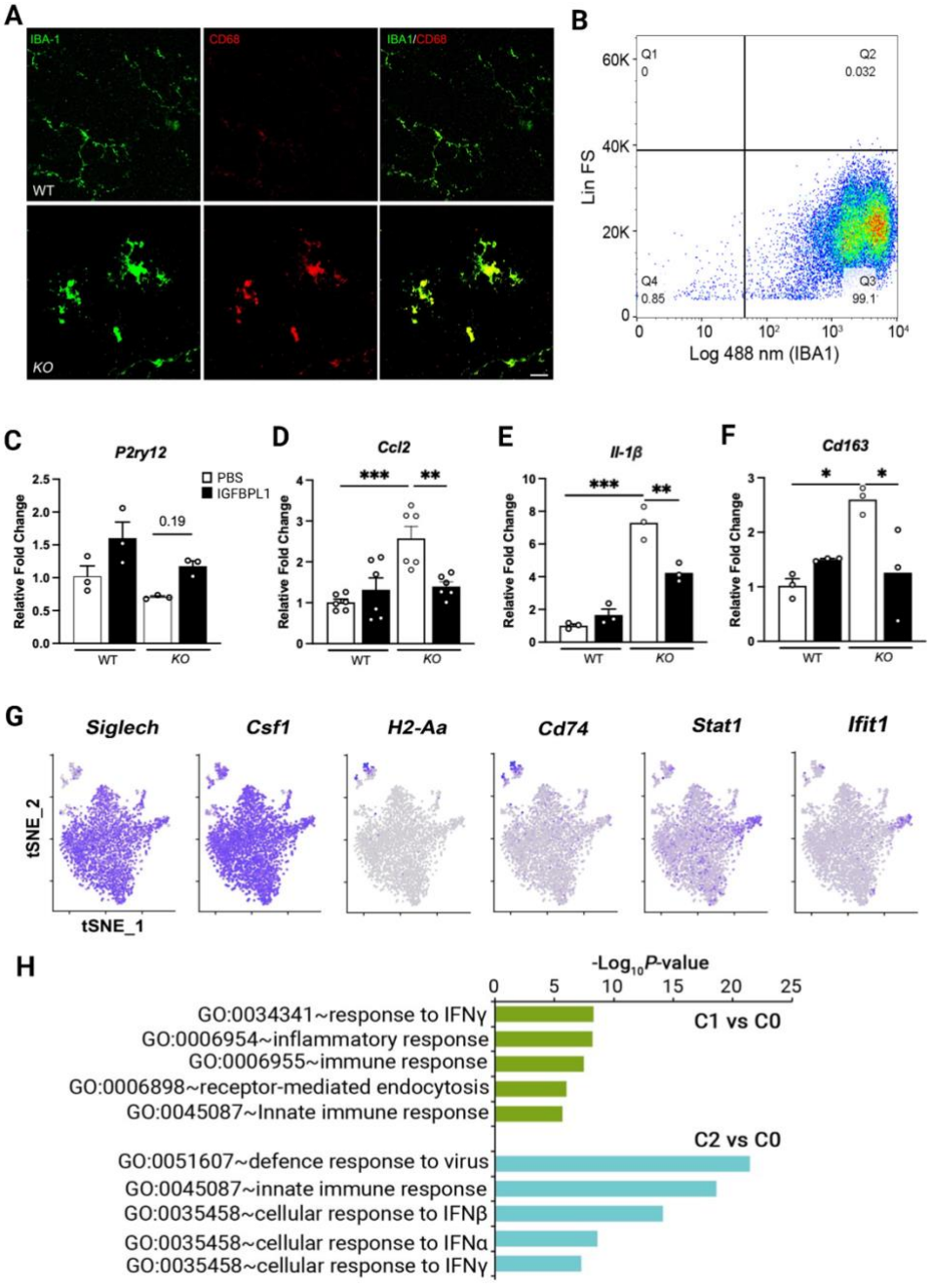

Figure S3. Upregulation of activated microglial markers in *KO* mice.

(A) Representative images of IBA-1^{+}CD68^{+} cells in retinal flat-mounts of WT and *KO* mice. Scale bar, 20μm.

(B) Representative plot presenting the FACS analysis of purity of isolated microglia which were labeled with anti-IBA-1.

(C-F) Results of qPCR showing relative mRNA levels of microglia markers *P2ry12* (C),

Ccl2 (D), *Il-1β* (E) and *Cd163* (F) in primary microglia isolated from WT and *KO* mice that were treated with PBS or IGFBPL1 for 48 hr. Relative fold change was normalized to the level of PBS treated WT brain microglia. *p<0.05, **p<0.01, ***p<0.001; One way ANOVA. n=3–6/group.

(G) tSNE plots of canonical retinal microglia genes detected in 7-month-old WT and *KO* retinas, including C0 resident microglial genes (*Siglech, Csf1*), C1 inflammatory microglial genes (*H2-Aa, Cd74*), C2 IFN-responsive pathway gene (*Stat1*) and C3 proliferating microglial gene (*Ifit1*).

(H) Bar chart representing pathways enriched in DEGs of C1 *vs* C0 and C2 *vs* C0 microglia, suggesting the inflammatory and/or IFNγ-responsive natures of C1 and C2 microglia.

Dots represent individual data. Data are mean±SEM.

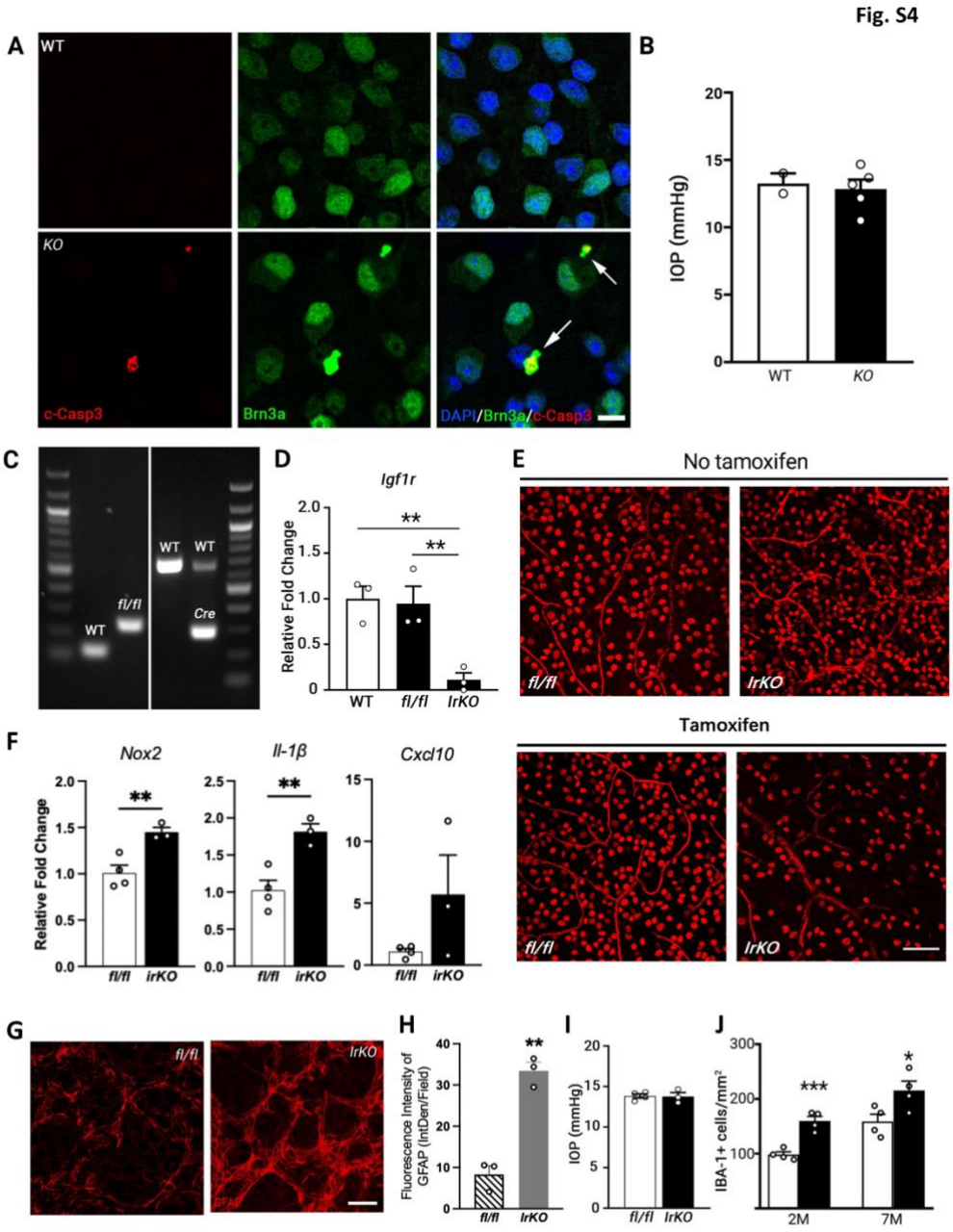

Figure S4. Deficiency of IGFBPL1 or IGF1r leads to glial activation and RGC loss without IOP elevation

(A) Representative images of double-immunolabeling for BRN3a and cleaved caspase-3 in retinal flat-mounts of WT and *KO* mice. Scale bar, 10μm.

(B) IOP levels in 10-month-old WT and *KO* mice (n=2 from WT mice; n=5 from *KO* mice).

(C) Representative gel images of PCR genotyping for WT, *fl/fl* (left panel) and $Cre^{+/-}$ (right panel) mice.

(D) qPCR results confirming minimal *Igf1r* expression in purified retinal microglial cells from tamoxifen-treated *IrKO* mice compared to WT and *fl/fl* mice. **p<0.01, One-way ANOVA with Tukey's multiple comparisons test (n=3 mice/group).

(E) Representative images of $BRN3a^{+}$ cells in retinal flat-mounts of adult *fl/fl* and *IrKO* littermates at 3-months after control or tamoxifen injection. Scale bar, 50µm.

(F) qPCR results showing significantly increased production of activated microglial marker (*Nox2*) and pro-inflammatory cytokines (*Il-1β, Cxcl10*) in *IrKO* retinas at 1-month post tamoxifen injection. **p<0.01, student's t test. (n>3 mice/group).

(G and H) Representative images (G) and quantifications (H) of GFAP immunostaining in retinal flat-mounts of *fl/fl* and *IrKO* littermates at 3-months post control or tamoxifen injection. Scale bar, 25µm.

(I) IOP levels measured in *fl/fl* and *IrKO* mice at 3 months after tamoxifen injection. *p<0.05, Student's t-test. n=4 mice/group.

(J) Counts of $IBA1^{+}$ cells in 2 and 7 months-old WT (white bar) and *KO* (black bar) mice. Dots represent individual mice. Data are mean±SEM.

Fig. S5

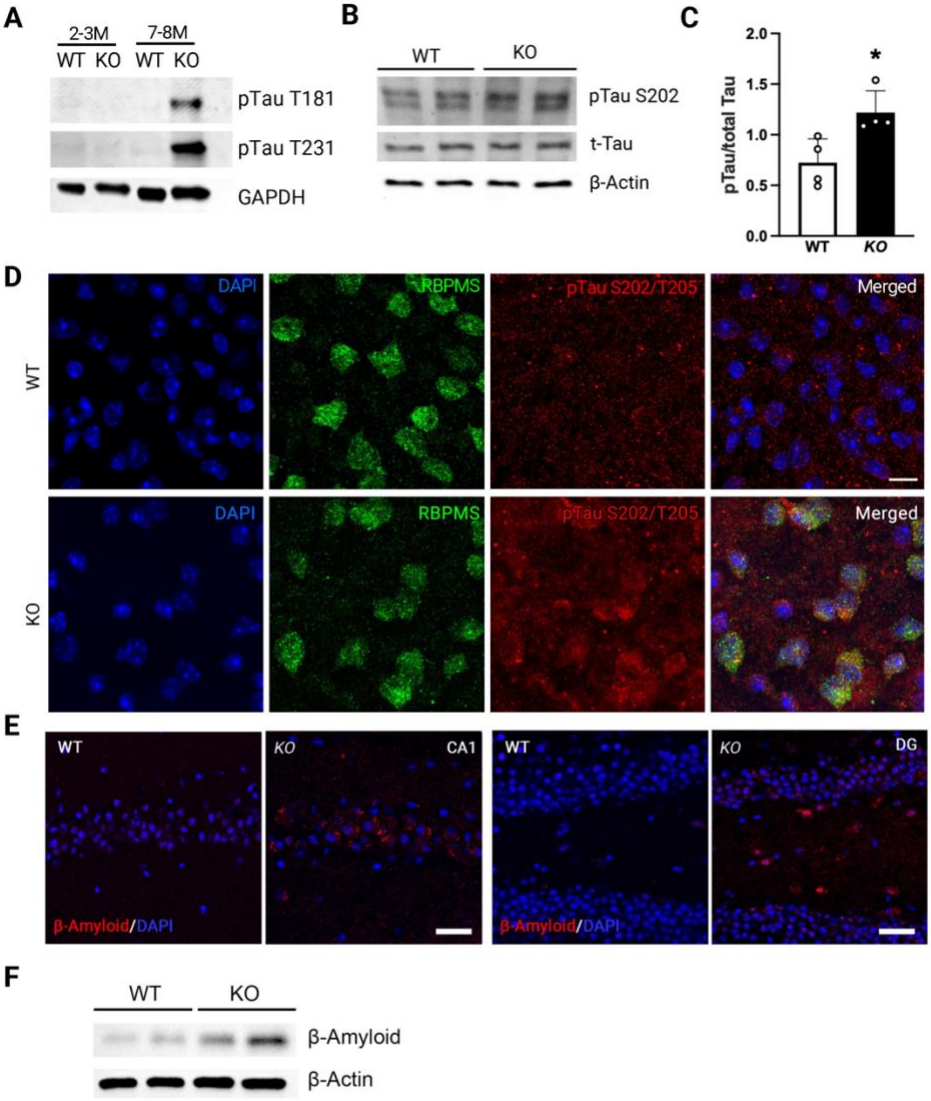

Figure S5. Accumulation of pTau and Aβ in *KO* mouse brains and retinas.

(A) Representative Western blot images of pTau T181/T231 in the hippocampus of WT and *KO* mice in 2-8 months of age.

(B and C) Representative Western blot (B) and densitometry analysis (C) of pTau S202/T205 in the retinal lysates from 7 months old retinas of WT and *KO* mice; both total Tau and β-actin were used as controls. Quantification of pTau S202/T205

expression in the retina of WT and *KO* mice is presented as fold changes relative to total Tau. *p<0.05, Student t-test. n=4 mice/group.

(D) Images of double-immunolabeling for pTau S202/T205 (red) and $RBPMS^{+}$ (green; an RGC marker) in WT and *KO* retinal flat-mounts that were counter-stained with a nuclei marker DAPI (blue). Scale bar, 50μm.

(E) Representative images of $A\beta_{1-42}$ immunolabeling in the hippocampus CA1 (CA1) region and dentate gyrus (DG) of hippocampus of 11-months-old WT and *KO* mice. Scale bar, 50μm.

(F) Representative Western blot images of β-amyloid in the hippocampus CA1 region and dentate gyrus of WT and *KO* mice.

Dots represent individual data. Data are mean±SEM.

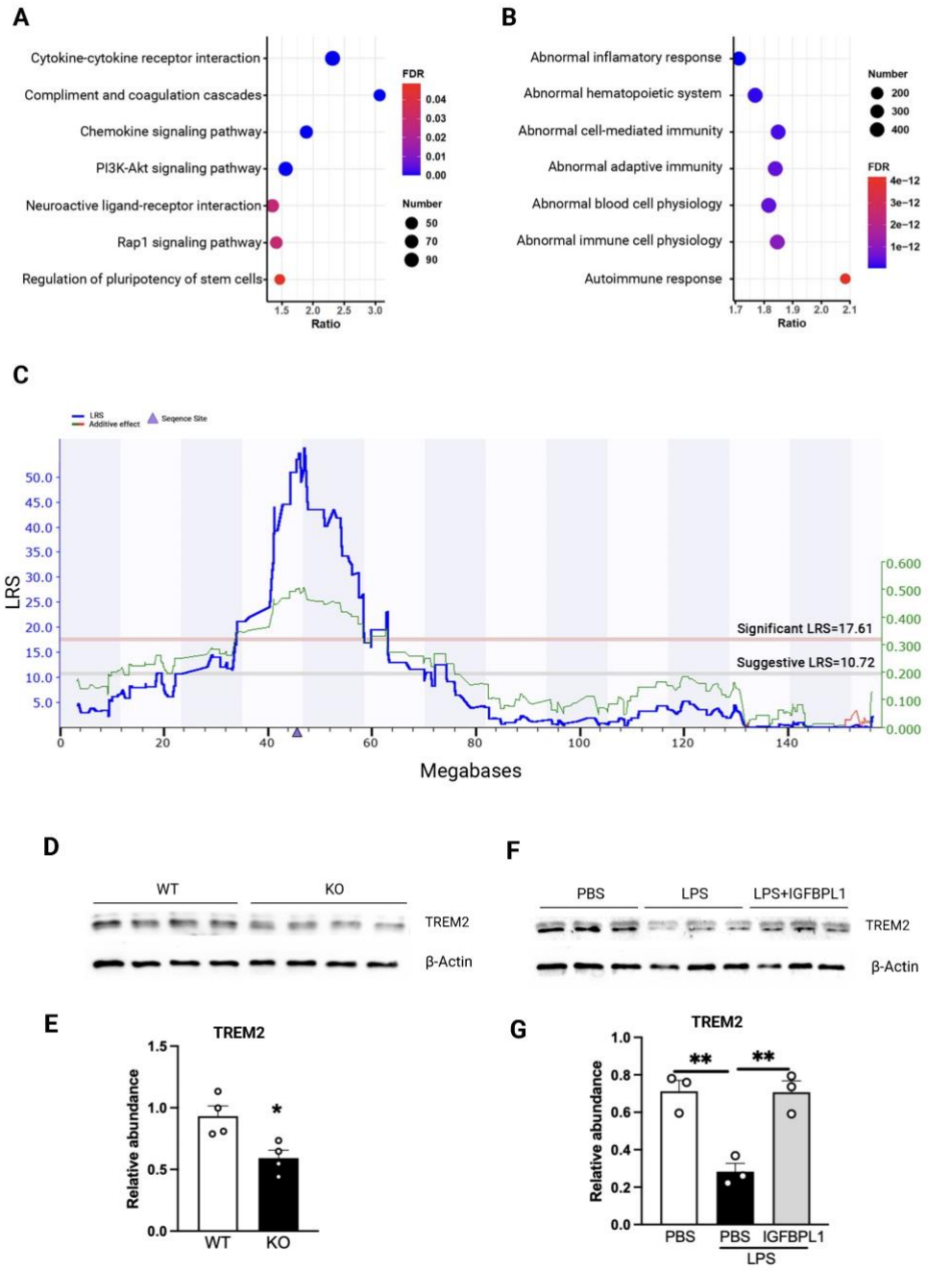

Figure S6. eQTL mapping of *Igfbpl1* in the eyes of aged BXD mouse strains and regulation of TREM2 expression.

(A,B) Dotplots of KEGG pathways (A) and Mammalian Phenotype Ontologies (B) enriched for *Igfbpl1* significantly correlated genes from RNA-seq data of aged BXD mouse eyes. The *x*-axis represents the enrich ratio and *y*-axis represents enriched pathways/terms. The size of the dots denotes the number of genes and the color the

p value.

(C) Manhattan plot showing a genome-wide significant eQTL in chromosome 4. The x-axis denotes the chromosomal position in megabases on the mouse genome, and y-axis indicates the LRS score. The pink and grey horizontal lines indicate significant and suggestive LRS, respectively. The purple triangle on the x-axis indicates the genomic position of Igfbpl1. LRS is shown by blue line, and additive effects are shown by green line.

(D-G) Representative Western blots (D,F) and quantification (E,G) of TREM2 expression in retinal lysates of 7 months-old WT and *KO* mice (D and E) or in primary microglia cultures treated with PBS, LPS (1µg/ml), LPS (1µg/ml) + IGFBPL1 for 24 hours (F and G). *p < 0.05, **p<0.01, one-way ANOVA with Tukey's multiple comparisons test. n=3–4 mice/group.

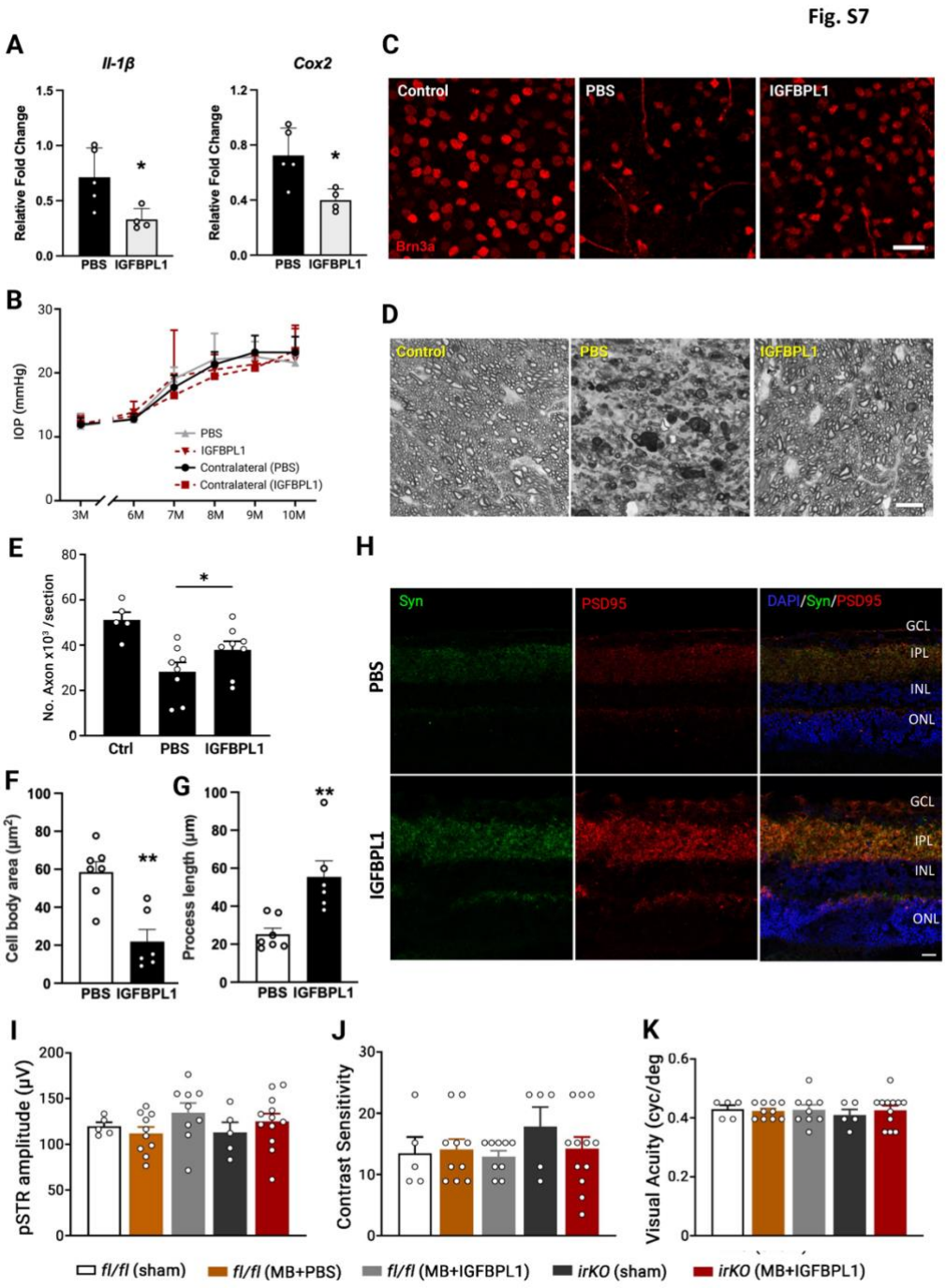

Figure S7. Treatment of IGFBPL1 mitigates neurodegeneration in DBA/2J and aged mice via IGF1R.

(A) Relative mRNA levels of *Il-1β* and *Cox2* in PBS- or IGFBPL1-treated retinas assessed at 3 weeks post MB-injection by qPCR. *p<0.05, Student's t test. n=4-5 mice/group.

(B) IOP profiles of DBA/2J mice in eyes ipsilateral and contralateral to eyes received

monthly intravitreal injections of PBS or IGFBPL1 (n=8 mice/group).

(C) Representative photomicrographs of BRN3a immunolabeled RGCs (red) in retinal flat-mounts from untreated 6 months-old (Ctrl) DBA/2J mice and 10-months-old DBA/2J mice received monthly treatment of PBS or IGFBPL1.

(D) Representative images of optic nerve cross-sections of untreated 6-month-old DBA/2J mice and 10-month-old DBA/2J mice with PBS or IGFBPL1 treatment. Scale bar, 10μm.

(E) Quantifications of axons in untreated 6-month-old DBA/2J mice and 10-month-old DBA/2J mice received PBS or IGFBPL1 treatment (n=8 mice/group). *$p<0.05$; One-way ANOVA with Tukey's multiple comparisons test.

(F and G) Quantification of microglial cell body area (F) and process length (G) in retinal flat-mounts of DBA2J mice received PBS or IGFBPL1 treatment. **$p<0.01$ Student's t test. n=6-7 mice/group.

(H) Representative images of retinal sections from 15 months-old WT mice received weekly PBS- or IGFBPL1-treatment for 4 weeks that were double-immunolabeled for PSD95 (red) and synapsin-I (Syn, green) and nuclei counter-stain (DAPI; blue). Scale bar, 15μm.

(I-K) The baseline measurements of pSTR amplitude (I), visual contrast sensitivity (J) and visual acuity (K) in *fl/fl* and *IrKO* mice with or without tamoxifen treatment. n=5–10 mice/group.

Dots represent individual data. Data are mean±SEM.

Table S1. qPCR primers used in this paper

Gene Name		Sequence
Igfbpl1	Forward	CTGTATGACCCTGGGCAAGT
	Reverse	GCCAGACCCAATTACGTGTT
Igf1	Forward	GTGGATGCTCTTCAGTTCGTGTG
	Reverse	TCCAGTCTCCTCAGATCACAGC
Igf-1r	Forward	CGGGATCTCATCAGCTTCACAG
	Reverse	TCCTTGTTCGGAGGCAGGTCTA
Cox2	Forward	GCGACATACTCAAGCAGGAGCA
	Reverse	AGTGGTAACCGCTCAGGTGTTG
Nox2	Forward	TGGCGATCTCAGCAAAAGGTGG
	Reverse	GTACTGTCCCACCTCCATCTTG
CD163	Forward	GGCTAGACGAAGTCATCTGCAC
	Reverse	CTTCGTTGGTCAGCCTCAGAGA
Tmem119	Forward	ACTACCCATCCTCGTTCCCTGA
	Reverse	TAGCAGCCAGAATGTCAGCCTG
Ccl2	Forward	CAA CTC TCA CTG AAG CCA G
	Reverse	TTA ACT GCA TCT GGC TGA G
Cxcl10	Forward	ATCATCCCTGCGAGCCTATCCT
	Reverse	GACCTTTTTTGGCTAAACGCTTTC
Il-1β	Forward	AAC CTG CTG GTG TGT GAC GTT C
	Reverse	CAG CAC GAG GCT TTT TTG TTG T
Il-1α	Forward	ACGGCTGAGTTTCAGTGAGACC
	Reverse	CACTCTGGTAGGTGTAAGGTGC
Iba-1	Forward	TCTGCCGTCCAAACTTGAAGCC
	Reverse	CTCTTCAGCTCTAGGTGGGTCT
Ym1	Forward	TACTCACTTCCACAGGAGCAGG

	Reverse	CTCCAGTGTAGCCATCCTTAGG
C1q	Forward	GTGGCTGAAGATGTCTGCCGAG
	Reverse	TTAAAACCTCGGATACCAGTCCG
Tnfα	Forward	TTCTCATTCCTGCTTGTGG
	Reverse	TTGGGAACTTCTCATCCCT
P21	Forward	TCGCTGTCTTGCACTCTGGTGT
	Reverse	CCAATCTGCGCTTGGAGTGATAG
Gapdh	Forward	CATCACTGCCACCCAGAAGACTG
	Reverse	ATGCCAGTGAGCTTCCCGTTCAG